Oncogene (2006) 25, 7618–7634

www.nature.com/onc

ORIGINAL ARTICLE

Imatinib enhances human melanoma cell susceptibility to TRAIL-induced cell death: relationship to Bcl-2 family and caspase activation

A Hamaï[1], C Richon[1], F Meslin[1], F Faure[2], A Kauffmann[3], Y Lecluse[4], A Jalil[1], L Larue[5], MF Avril[4], S Chouaib[1] and M Mehrpour[1,6]

[1]*INSERM, U753, Laboratoire d'Immunologie des Tumeurs Humaines: Interaction effecteurs cytotoxiques-système tumoral, Institut Gustave Roussy PR1 and IFR 54, Villejuif, France;* [2]*INSERM, U520, laboratoire de biologie cellulaire de l'immunité antitumorale, Institut Curie, Paris, France;* [3]*CNRS, UMR 8125, laboratoire de Génétique Oncologique, Institut Gustave Roussy PR1, Villejuif, France;* [4]*Institut Gustave Roussy PR2, Villejuif, France;* [5]*CNRS, UMR 146, Génétique du développement des mélanocytes, Institut Curie, Orsay, France and* [6]*Chinese Academy of Sciences, Laboratory of Apoptosis and Cancer Biology, The National Key Laboratory of Biomembrane and Membrane Biotechnology, Institute of Zoology, Beijing, China*

In order to define genetic determinants of primary and metastatic melanoma cell susceptibility to tumor necrosis factor-related apoptosis-inducing ligand (TRAIL), we have applied oligonucleotide microarrays to TRAIL-sensitive primary T1 cells and TRAIL-resistant metastatic G1 cells treated or not with TRAIL. T1 and G1 cells are isogenic melanoma cell subclones. We examined 22 000 spots, 4.2% of which displayed differential expression in G1 and T1 cells. Cell susceptibility to TRAIL-mediated apoptosis was found to be correlated with gene expression signatures in this model. Some of the differentially expressed genes were identified as involved in ATP-binding and signaling pathways, based on previously published data. Further analysis provided evidences that c-kit was overexpressed in G1 cells while it was absent in T1 cells. The c-kit inhibitor, imatinib, did not restore TRAIL sensitivity, excluding a role for c-kit in TRAIL resistance in G1 cells. Surprisingly, imatinib inhibited cell proliferation and TRAIL-mediated apoptosis in melanoma cells. We investigated the possible involvement of several molecules, including c-ABL, platelet-derived growth factor receptor (PDGFR), cellular FADD-like interleukin-1 α-converting enzyme-like inhibitory protein (c-FLIP)$_{L/S}$, Fas-associated DD kinase, p53, p21^{WAF1}, proteins of B-cell leukemia/lymphoma 2 (Bcl-2) family and cytochrome *c*. Imatinib did not modulate the expression or activation of its own targets, such as c-ABL, PDGFRα and PDGFR*β*, but it did affect the expression of c-FLIP$_L$, BCL2-associated X protein (Bax) and Bcl-2. Moreover, c-FLIP$_L$ knockdown sensitized T1 cells to TRAIL-mediated apoptosis, with a sensitivity similar to that of cells previously treated with imatinib. More notably, we found that the resistance to TRAIL in G1 cells was correlated with constitutive c-FLIP$_L$ recruitment to the DISC and the inhibition of caspase 8, 3 and 9 processing. Moreover, c-FLIP$_L$ knockdown partly restored TRAIL sensitivity in G1 cells, indicating that the expression level of c-FLIP$_L$ and its interaction with TRAIL receptor2 play a crucial role in determining TRAIL resistance in metastatic melanoma cells. Our results also show that imatinib enhances TRAIL-induced cell death independently of BH3-interacting domain death agonist translocation, in a process involving the Bax:Bcl-X$_L$ ratio, Bax:Bcl-X$_L$/Bcl-2 translocation, cytochrome *c* release and caspase activation. Our data indicate that imatinib sensitizes T1 cells by directly downregulating c-FLIP$_L$, with the use of an alternative pathway for antitumor activity, because PDGFRα is not activated in T1 cells and these cells do not express c-kit, c-ABL or PDGFR*β*. Caspase cascade activation and mitochondria also play a key role in the imatinib-mediated sensitization of melanoma cells to the proapoptotic action of TRAIL.
Oncogene (2006) **25,** 7618–7634. doi:10.1038/sj.onc.1209738; published online 18 September 2006

Keywords: human melanoma; metastasis; apoptosis; gene expression profiling; TRAIL; tyrosine kinase

Introduction

The resistance of melanoma to therapeutic treatment, together with its strong tendency to metastasize, represents a major clinical obstacle to treatment. Recent genomic studies have identified genes (*WNT5A*, *BRAF*, *RHO-C*) for which expression or mutation is correlated with melanoma progression, but melanoma continues to be an unpredictable cancer (Bittner *et al*., 2000; Clark *et al*., 2000; Carr *et al*., 2003). Serial analysis of gene expression in melanoma tumors has shown that intracellular calcium levels, G-protein signaling and *HLA DG* expression are upregulated (Weeraratna *et al*., 2004). However, changes at the genomic, transcriptional and post-translational levels for G-proteins and protein kinases (RAS, BRAF) and their transcription factor

Correspondence: Dr M Mehrpour, INSERM, U753, Laboratoire d'Immunologie des tumeurs Humaines : Interaction effecteurs cytotoxiques-système tumoral, Institut Gustave Roussy, PR1, F-94805 Villejuif Cedex, France.
E-mail: mehrpour@igr.fr or mehrpour@ioz.ac.cn
Received 22 July 2005; revised 24 March 2006; accepted 9 May 2006; published online 18 September 2006

effectors (AP2, c-JUN, ATF2, STAT3 and NF-*k*B) also affect death domain receptors in the acquisition of resistance to apoptosis in melanoma cells (for reviews see Hersey and Zhang, 2001; Ivanov *et al*., 2003; Soengas and Lowe, 2003).

Tumor necrosis factor-related apoptosis-inducing ligand (TRAIL) is normally present as a trimeric type II transmembrane protein on various immune effector cells. It specifically induces apoptosis in cancer cells with no apparent apoptotic activity towards normal cells. However, many cancers cells, including the cells of some highly malignant tumors, are resistant to apoptosis induction by TRAIL. Such resistance may occur at various points in the TRAIL-induced apoptosis signaling pathways. An understanding of molecular mechanisms underlying such resistance and the development of strategies to overcome it are essential for the successful use of TRAIL to treat melanoma.

Homotrimeric TRAIL initiates apoptosis after cross-linking of the agonistic receptors TRAIL receptor (TRAIL-R)1 (death receptor (DR)4) and TRAIL-R2 (DR5), leading to activation of the extrinsic apoptotic pathway via the death-inducing signaling complex (DISC) (for reviews see Wang and El-Deiry, 2003; Debatin and Krammer, 2004; Yagita *et al*., 2004). Assembly of the DISC subsequently activates initiator caspases (caspase 8 or 10) and effector caspases (caspase 3 or 7), ultimately leading to apoptotic cell death (Hasegawa *et al*., 1996). Two additional receptors were identified as TRAIL-R3 (decoy receptors (DcR1)) and TRAIL-R4 (DcR2). These receptors have incomplete cytoplasmic death domains or lack such domains entirely, and are thought to inhibit TRAIL-induced apoptosis by acting as DcRs (LeBlanc and Ashkenazi, 2003). The TRAIL-induced apoptosis of melanoma cells also involves the intrinsic mitochondrial pathway (Thomas *et al*., 1998). The mitochondrial network, which can be initiated by various death signals, triggers the release of apoptogenic factors, such as cytochrome *c*, from mitochondria. In the cytoplasm, cytochrome *c* binds to APAF-1, leading to the activation of caspase 9, which in turn activates caspase 3 (Kroemer *et al*., 1997). B-cell leukemia/lymphoma 2 (Bcl-2) family members control the mitochondrial response to apoptotic stimuli (for a review see Gross *et al*., 1999). Antiapoptotic Bcl-2 family members (Bcl-2 and Bcl-X_L) maintain mitochondrial membrane integrity, whereas multidomain pro-apoptotic proteins (e.g. BCL2-associated X protein (Bax) and Bak) facilitate the release of apoptogenic factors from mitochondria, initiating the caspase cascade and organelle dysfunction. BH3-interacting domain death agonist (Bid) is a unique proapoptotic member of the Bcl-2 family in that once activated by caspase 8, its C-terminal domain (tBid) can be translocated into mitochondria (Hodgkinson *et al*., 1993), inducing the oligomerization of Bax or Bak (Desagher *et al*., 1999; Wei *et al*., 2000). This results in permeabilization of the outer mitochondrial membrane and cytochrome *c* release. The activation of Bid by caspase 8 therefore provides a bridge between the extrinsic and intrinsic apoptotic pathways.

Several recombinant forms of TRAIL with strong tumorigenic activity *in vitro* and in animal models but with no toxic side effects have been generated (Ashkenazi *et al*., 1999; Walczak *et al*., 1999; Kelley *et al*., 2001), suggesting a possible role for TRAIL in human cancer therapy. However, other studies have reported the induction by TRAIL of apoptotic activity in some normal human cells (Leverkus *et al*., 2000; Nesterov *et al*., 2002).

TRAIL and DNA-damaging therapies such as chemotherapeutic drugs or ionizing irradiation have been reported to display strong synergistic apoptotic activity (Muhlethaler-Mottet *et al*., 2004; Wendt *et al*., 2005; Yamaguchi *et al*., 2005). A similar phenomenon is observed with various inhibitors, including inhibitors of the Na^+/H^+ antiporter (Kim and Lee, 2005), of the epidermal growth factor receptor (EGFR) (Ivanov and Hei, 2005), or the tyrosine kinase inhibitor, imatinib, in Bcr-Abl-positive human acute leukemia cells (Nimmanapalli and Bhalla, 2002). The pharmacological compound imatinib (formerly known as CGP 57148B, STI571, or Gleevec) is a 2-phenylamino-pyrimidine derivative that inhibits the tyrosine kinase activities of kinases such as c-ABL, platelet-derived growth factor receptors (PDGFRs) and c-kit, in several systems (Carroll *et al*., 1997; Heinrich *et al*., 2000; Krystal *et al*., 2000; Druker, 2002; Lefevre *et al*., 2004). Imatinib has also been shown to inhibit effectively the closely related FMS receptor for macrophage colony-stimulating factor (Taylor *et al*., 2006).

The aim of this study was to determine the molecular basis of the susceptibility to TRAIL-mediated apoptosis of primary and metastatic melanoma cells. We identified differentially expressed genes critical to the resistance of metastatic cells to TRAIL-induced apoptosis and showed that imatinib increased the TRAIL-induced apoptosis of primary melanoma cells. The mechanisms associated with imatinib-induced enhancement of human melanoma cell susceptibility to TRAIL-induced apoptosis appear to involve cellular FADD-like interleukin-1 α-converting enzyme-like inhibitory protein (c-$FLIP)_L$, the Bcl-2 family and caspase cascade activation.

Results

G1 metastatic melanoma cells are more resistant to TRAIL-induced apoptosis than T1 primary melanoma cells

An analysis of the sensitivity of G1 and T1 tumor cells to TRAIL-mediated apoptosis showed that G1 cells were resistant to TRAIL-mediated cell death (only $25\% \pm 5$ apoptotic cells), whereas T1 cells displayed strong dose- and time-dependent sensitivity to TRAIL (Figure 1). The effect was maximal for cells exposed to 1 μg/ml of TRAIL for 48 h (P-value <0.01, 60% apoptotic cells) (Figure 1a). We investigated the difference in sensitivity to TRAIL-mediated apoptosis

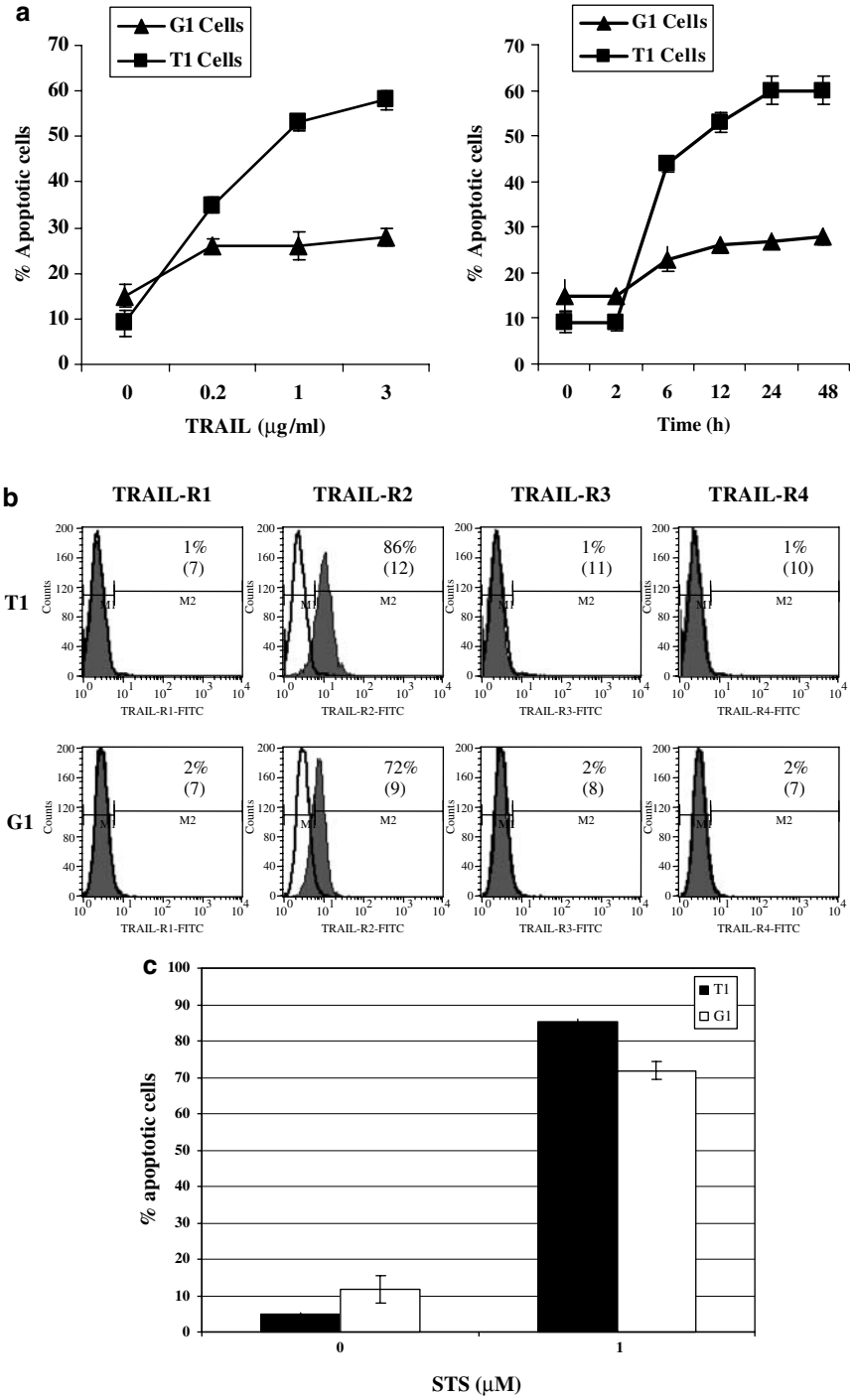

Figure 1 Sensitivity of metastatic G1 and primary T1 cells to TRAIL-mediated apoptosis. (**a**) Cells were exposed to the indicated concentration of TRAIL for 48 h. Cells were also exposed to 1 μg/ml TRAIL for the time. Apoptotic cells were identified as Annexin V+ cells. (**b**) Expression of the TRAIL receptors on T1 and G1 cells was determined by indirect immunofluorescence analysis, using anti-TRAIL-R1 (M271 clone), anti-TRAIL-R2 (M413 clone), anti-TRAIL-R3 (M430 clone) and anti-TRAIL-R4 (M445 clone) (gray curve). Isotypic IgG1 (negative control) was included (open curve). The level of cell surface expression is indicated by the shift of the gray curve to the right from the open control curve. Black numbers indicate percentages of positive cells. Numbers in brackets indicate mean fluorescence intensity. Results are representative of three independent experiments. (**c**) Cells were exposed to staurosporine (STS; 1 μM) for 4 h. The percentage of cells undergoing apoptosis was determined by $DiOC_6(3)$ and PI staining, followed by flow cytometry.

between G1 and T1 cells, by carrying out immunofluorescence analysis with anti-TRAIL-R1/DR4, anti-TRAIL-R2/DR5, anti-TRAIL-R3/DcR1 and anti-TRAIL-R4/DcR2 monoclonal antibodies. Both cell types expressed TRAIL-R2 on their surface (Figure 1b), suggesting that the resistance of G1 cells to TRAIL-mediated apoptosis was not due to a lack of expression of TRAIL receptors.

The mitochondrial pathway has been reported to be involved in the TRAIL-induced apoptosis of melanoma cells. We therefore investigated the possible involvement of this pathway in TRAIL-resistant melanoma cells. We used staurosporine (a PKC inhibitor) to induce apoptosis through the intrinsic pathway. The data depicted in Figure 1c indicated that both cell lines exhibit a high sensitivity to staurosporine suggesting that the resistance of G1 cells to TRAIL-mediated apoptosis was also independent from the mitochondrial (or postmitochondrial) level.

Gene expression profiling in TRAIL-resistant metastatic G1 and primary TRAIL-sensitive T1 melanoma cells

We investigated the molecular basis of the resistance of metastatic melanoma G1 cells to TRAIL-mediated apoptosis, by studying global gene expression in the G1/T1 cell model, using oligonucleotide microarrays. RNA samples were prepared from TRAIL-resistant metastatic G1 and TRAIL-sensitive primary T1-cell lines with and without TRAIL (0.2 and 1 μg/ml) treatment for 24 h. Principal component analysis (PCA) of the data set indicated effective discrimination between the TRAIL-sensitive T1 and TRAIL-resistant G1-cell lines (Figure 2a). Our data correctly separated all the PCA plots for T1 from all the PCA plots for G1 cells. It was possible to separate untreated T1 from treated T1 cells by this method, whereas the PCA plots of treated and untreated G1 cells were essentially similar. Thus, cell susceptibility to TRAIL-mediated apoptosis and gene expression signatures were strongly correlated.

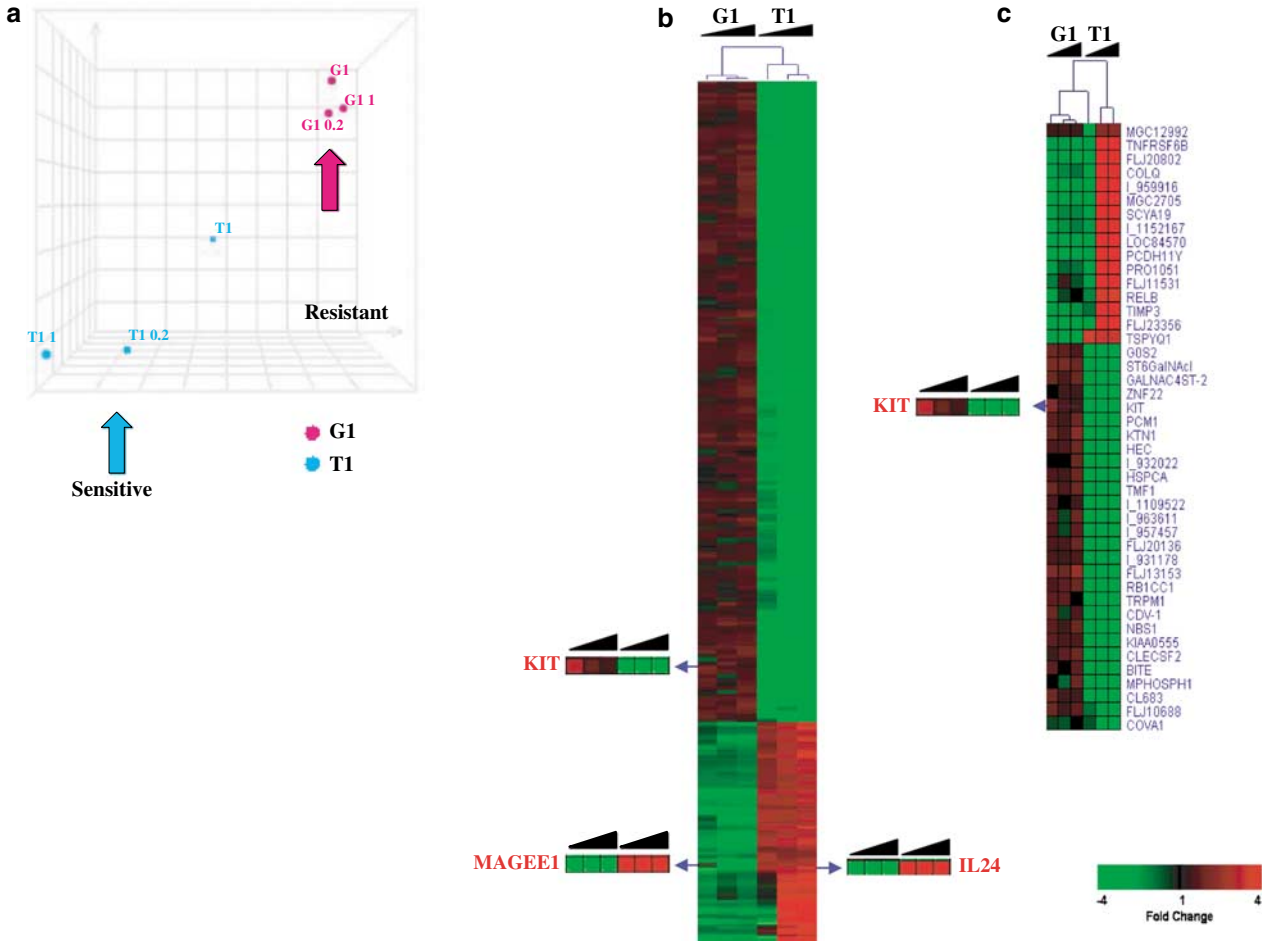

Figure 2 PCA, hierarchical clustering and gene ontology functional classification of gene expression for genes differentially expressed in metastatic TRAIL-resistant G1 and primary TRAIL-sensitive T1 cells. (**a**) PCA plot. The three-dimensional plot shows the significant discriminating genes for each cell line and TRAIL treatment in the three principal axes. Blue circles indicate the genes of untreated T1 cells (T1) and of T1 cells treated with 0.2 and 1 μg/ml TRAIL (T1 0.2 and T1 1), respectively; pink circles indicate the genes of untreated G1 cells (G1) and G1 cells treated with 0.2 and 1 μg/ml TRAIL (G1 0.2 and G1 1). (**b**) ANOVA was used (see Materials and methods) to identify genes differentially expressed in G1 and T1 cells, with or without treatment (P-value $< 10^{-15}$). For clustering analysis, we used the Cluster and Tree initialization of the Rosetta Resolver software package. The dendogram based on pairwise calculations of the Pearson correlation coefficient shows the $\log_2$-converted hybridization ratio of fluorescent cRNA probes prepared from each experimental RNA (test) to the reference RNA (pool of all sample). The intensity of the squares reflects the fold repression (green) or fold-induction (red), according to the color scale at the top (where black indicates no significant change in gene expression). Each column represents a single hybridization experiment between the test and reference samples. The first and fourth column correspond to G1 and T1 cells; the second, third, fifth and sixth columns correspond to G1 and T1 cells treated with 0.2 and 1 μg/ml TRAIL for 24 h, respectively. Each row represents the expression pattern of a single gene in the various experiments. This dataset can be found in our Supplementary Data. (**c**) The discriminating genes for TRAIL treatment, identified by ANOVA ($P < 10^{-15}$). Data are shown as in (**b**).

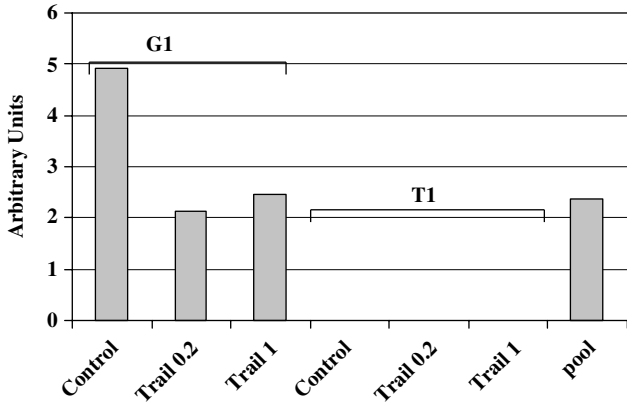

Figure 3 *KIT* expression in metastatic TRAIL-resistant G1 and primary TRAIL-sensitive T1 cells. *KIT* gene expression in metastatic TRAIL-resistant G1 and primary TRAIL-sensitive T1-cell lines was assessed by quantitative RT–PCR. Results are expressed as the mean ± s.d. for three independent determinations (***$P<0.001$).

We then analysed the data by two-way ANOVA with *P*-values $\leqslant 10^{-15}$ considered significant. The two factors included in the analysis were cell line (Figure 2b) and TRAIL treatment (Figure 2c). This analysis distinguished between the TRAIL-resistant G1 and the TRAIL-sensitive T1-cell lines and led to the identification of 966 discriminating genes from a total of 22 000 spots (see Supplementary Data). Hierarchical cluster analysis and gene dendrograms generated showed that, in the untreated cells, 694 genes were induced by a factor of 1.5 to 56, and 193 genes were repressed, by a factor of 1.5–38 (Figure 2b). We also identified 37 genes showing slight induction (factor of 1–1.5) and 42 displaying slight repression (factor of 1- to 1.5-fold) in untreated cells, but the expression patterns of these genes became more marked in samples treated with TRAIL. We cannot describe in detail all the genes found to be differentially expressed here but we focus on some of them below. Real-time RT–PCR analysis for some genes (*MAGEE1 and IL24*) confirmed the differential pattern

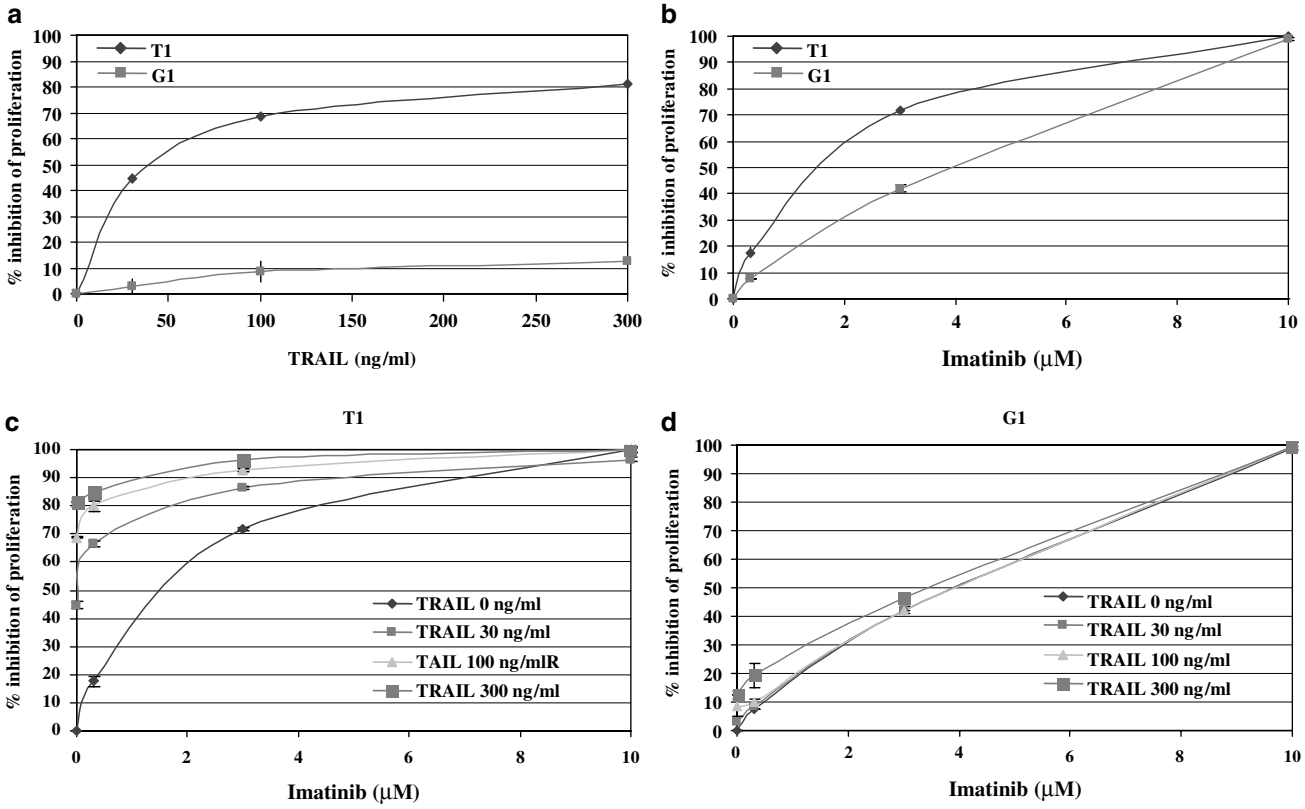

Figure 4 Effect of TRAIL, imatinib or TRAIL-imatinib cotreatment on proliferation and apoptosis of melanoma cells. (**a**) T1 and G1 cells were cultured with various doses of TRAIL and (**b**) imatinib for 48 h. (**c**) T1 cells and (**d**) G1 cells were cultured with the indicated combinations of TRAIL and imatinib for 48 h. Results are expressed as percentage proliferation inhibition (%) = (c.p.m. (untreated)–c.p.m. (treated))/c.p.m. (untreated). (**e**) Imatinib increased TRAIL-induced cell death in a dose-dependent manner. T1 (top) and G1 (bottom) cells were incubated with or without the indicated concentrations of imatinib for 24 h and then with or without the indicated concentrations of TRAIL for 12 h. Apoptosis was evaluated by $DiOC_6(3)$ and PI staining and FACS analysis. All data were expressed as mean ± s.d. from two individual experiments. (**f**) Imatinib increased TRAIL-induced cell death in a dose-dependent manner in other melanoma cell lines. M10, MT10, and MG10 cells were incubated with or without the indicated concentrations of imatinib for 24 h and then with or without the indicated concentrations of TRAIL for 48 h. Apoptosis was evaluated as described in (**e**). All data were expressed as mean ± s.d. from two individual experiments.

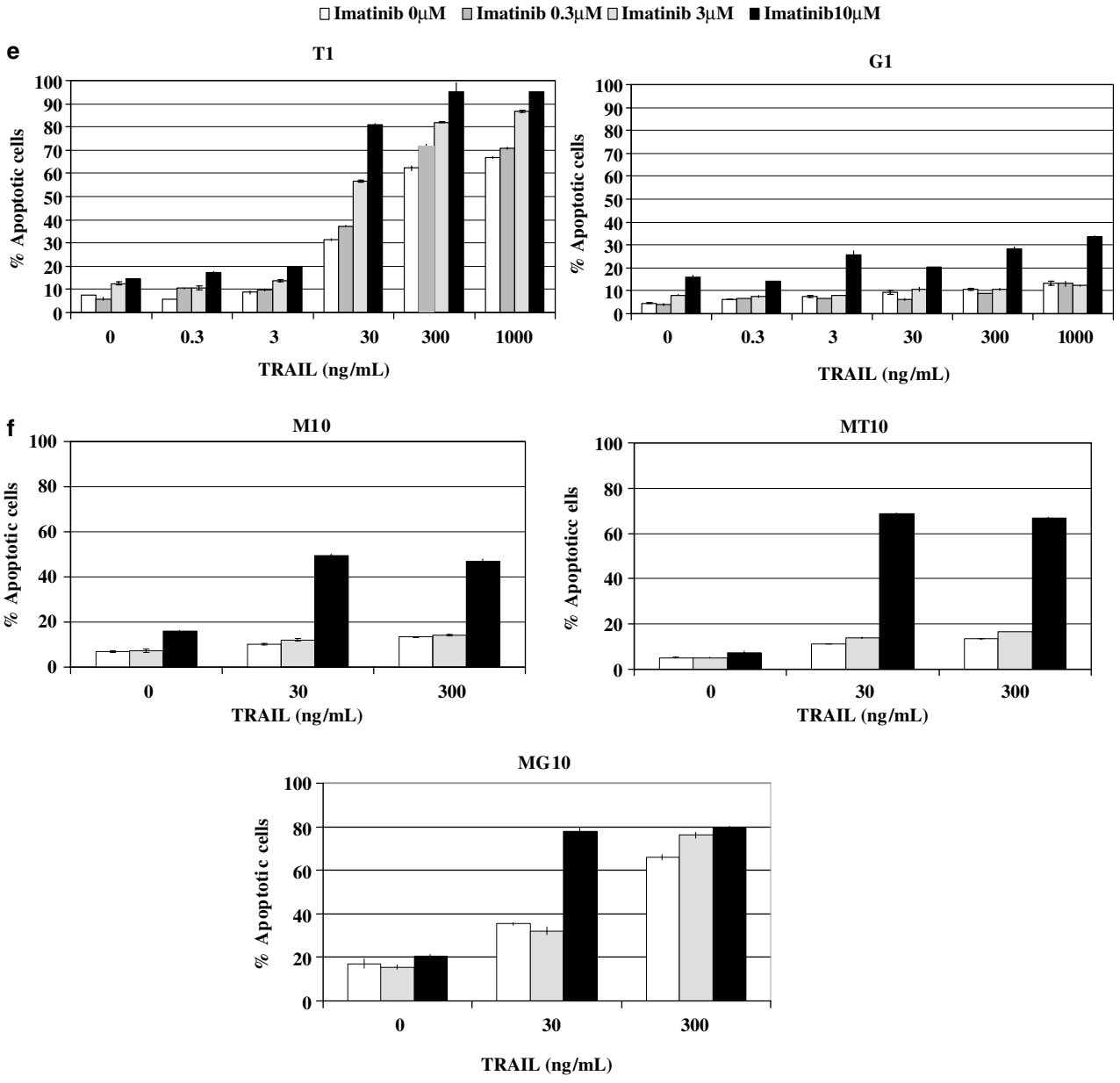

Figure 4 *Continued.*

of gene expression identified by microarray (data not shown). We investigated the potential importance of each gene and tried to identify the genes most likely to be associated with the acquisition of TRAIL resistance by metastatic tumor cells, by clustering the expressed genes into subgroups according to biological processes or molecular functions, as determined from gene ontology vocabularies (given in Figure 2d and e in Supplementary Data), using the Fatigo web tool (Al-Shahrour *et al*., 2004). Various intracellular signaling pathways are affected during the acquisition of TRAIL resistance and human melanoma progression (Figure 2d and e in Supplementary Data). The lower *P*-value (***P-value <0.0001) was obtained for the adenyl nucleotide-binding group. Two subgroups emerged in this group: genes encoding proteins with protein kinase activity (tyrosine and serine/threonine) and genes encoding proteins associated with ATPase activity. This suggests that ATP binding may be affected during the acquisition of TRAIL resistance and human melanoma progression.

ANOVA analysis (P-value $\leqslant 10^{-15}$) for the effect of TRAIL treatment identified 44 discriminating genes. Hierarchical cluster analysis and gene dendrograms generated is depicted in the Figure 2c. These genes were grouped into two clusters, with the exception of two genes with distinct expression profiles. The first of these genes, *MGC12992,* displayed similar levels of expression in treated and untreated G1 cells, but was downregulated in untreated T1 cells and upregulated in TRAIL-treated T1 cells. The second gene, *TSPYQ1*, displayed down-

regulation in G1 cells and upregulation in T1 cells. The first cluster consisted of 14 genes that were downregulated in G1 cells; in T1 cells, these genes were downregulated in the absence of treatment and upregulated following TRAIL treatment. The second cluster consisted of 28 genes that were upregulated in G1 cells and downregulated in T1 cells, with TRAIL treatment having little effect. These 44 discriminating genes were also grouped into functional categories, according to data from the Gene Ontology database. Four genes (*HSPCA* encoding Hsp90, *FLJ23356*, *MPHOSPH1* encoding M-phase phosphoprotein 1, and *KIT*) were associated with ATP binding, two of which were also associated with protein tyrosine kinase activity (*KIT* and *FLJ23356*); three genes (*MPHOSPH1*, *NBS1* and *G0S2*) were associated with the cell cycle and another three genes (*PCM1*, *TMF1* and *ZNF22*) were associated with DNA binding. Our results suggest that the protein tyrosine kinase signaling pathway may interfere with metastatic tumor cell resistance to the proapoptotic action of TRAIL. Hierarchical and K-mean clustering analyses were carried out (number of clusters: 5; maximum number of iterations: 50) and gene dendograms generated for all the kinases differentially expressed in T1 and G1 cells (from the total of 966 discriminating genes; Figure 2f in Supplementary Data). These genes were grouped into two clusters (up- or downregulated in G1 cells, with respect to levels of expression in T1 cells). Using Fatiwise web tool (Al-Shahrour *et al*., 2004), we found that these kinases belong to various pathways, including transmembrane receptor signaling, tyrosine kinase activity, the cell cycle, apoptosis, mitogen-activated protein kinase (MAPK) signaling, Toll-like receptor signaling, phosphatidylinositol signaling and Jak-Stat signaling.

KIT *overexpression in metastatic tumor cells*

Oligonucleotide microarray analysis identified *KIT* as discriminating between the G1- and T1-cell lines (expression level 2.5 times higher in G1 cells and 18 times higher in T1 cells than in the pool) and involved in the signaling pathway before and after TRAIL treatment. We therefore carried out real-time quantitative RT–PCR analysis to quantify this differential expression. *KIT* expression was undetectable in T1 cells, whereas it was upregulated (2.5 times higher than for the pool) in G1 cells (Figure 3). In addition, immunofluorescence analysis with an anti-human c-kit monoclonal antibody indicated that c-kit was present on the surface of G1 cells but not on the surface of T1 cells (data not shown). These results confirm that c-kit is expressed at both mRNA and protein levels only in metastatic TRAIL-resistant cell line as compared to primary TRAIL-sensitive cell line.

Imatinib treatment alone prevents melanoma cell proliferation

As *KIT* was found to be overexpressed in G1 cells and absent from T1 cells, it was identified as a gene discriminating between the G1- and T1-cell lines and involved in signaling before and after TRAIL treatment. We therefore inhibited the tyrosine kinase receptor encoded by this gene with imatinib, to determine it was involved in the resistance of G1 cells to the cytotoxic action of TRAIL. For this purpose, we cultured cells with various concentrations of imatinib, TRAIL and a combination of both, for 48 h. Imatinib inhibited the proliferation of G1 cells in a dose-dependent manner, even though TRAIL had no effect (Figure 4a and b). The concentration giving 50% growth inhibition (IC50) of imatinib was about 4 μM. Surprisingly, despite the absence of c-kit expression in T1 cells, imatinib also inhibited the proliferation of T1 cells in a dose-dependent manner (IC50, 1.6 μM), and T1 cells were more sensitive than G1 cells to the effects of this drug (Figure 4a and b). This suggests that the inhibition of melanoma cells proliferation by imatinib may be independent of c-kit expression. Strong growth inhibition (P-value <0.01, 90%) was observed if T1 cells were treated with both TRAIL and imatinib (Figure 4c), whereas this treatment had no effect on G1 cells (Figure 4d).

Figure 5 Combining TRAIL and imatinib enhances caspase and PARP cleavage. (**a**) Imatinib treatment did not modify expression and phosphorylation state of PDGFRα, PDGFRβ and c-ABL during TRAIL-induced-cell death in T1 cells. T1 cells were incubated for 24 h with or without 3 μM imatinib and were then treated with or without 300 ng/ml TRAIL for the indicated times. Cell lysates were subjected to SDS–PAGE, blotted and probed with antibodies, as indicated. K562 cell lysate was used as a positive control and phosphorylation of c-ABL. 3T3 cell lysate was used as a positive control for expression and phosphorylation of PDGFRα, and CCD-1064Sk (sc-2264) and CCD-1064Sk-PDGFR (sc-2263) cell lysates were used as negative and positive controls, respectively, for the expression and phosphorylation of PDGRFβ. The corresponding actin or nonspecific band (NS) levels are shown as loading controls. (**b**) Cells were incubated for 24 h with or without 3 μM imatinib and were then treated with or without 300 ng/ml TRAIL for 14 h. TRAIL receptor expression was determined by indirect immunofluorescence analysis, using anti-TRAIL-R1, anti-TRAIL-R2, anti-TRAIL-R3 and anti-TRAIL-R4 antibodies. (**c**) Cells were incubated for 24 h with or without 3 μM imatinib and then with or without 300 ng/ml TRAIL for the indicated times. Whole-cell lysates were subjected to SDS–PAGE, blotted and probed with antibodies recognizing full-length and cleaved forms of caspase 3, 8 and 9 proteins. The sizes of the signature proteolytic fragments are shown on the left. The figure is representative of two to three similar independent experiments. (**d**) Confocal microscopy analysis of cleaved PARP and cleaved caspase 3 localization. T1 cells were cultured in the presence or absence of imatinib (3 μM) overnight and were then treated with TRAIL (300 ng/ml) or with a combination of imatinib and TRAIL for 4 h, followed by immunofluorescence staining with antibodies recognizing cleaved PARP or caspase 3. Nuclei were counterstained with Topro-3. The confocal scanning fluorescence micrographs are representative of most of the cells analysed. In parallel, T1 and G1 cells were incubated overnight with or without 3 μM imatinib and then with or without 300 ng/ml TRAIL for 4 h. Cell lysates were subjected to SDS–PAGE, blotted and probed with PARP antibody (cleaved form). The corresponding nonspecific band (NS) levels are shown as loading controls.

Imatinib enhances TRAIL-mediated apoptosis in melanoma cells

As imatinib inhibited the proliferation of melanoma cells, we investigated its possible effects on the TRAIL-induced apoptosis of these cells. We determined the dose-dependent response to imatinib combined with TRAIL, by direct determination of mitochondrial transmembrane potential ($\Delta\psi 7$ m) with $DiOC_6$. Imatinib alone did

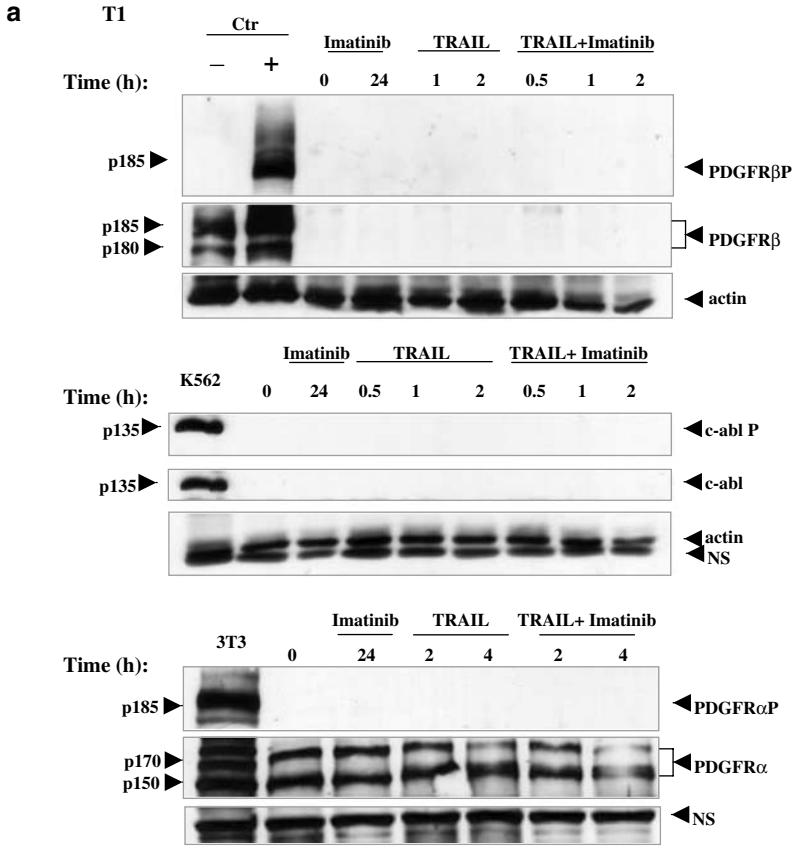

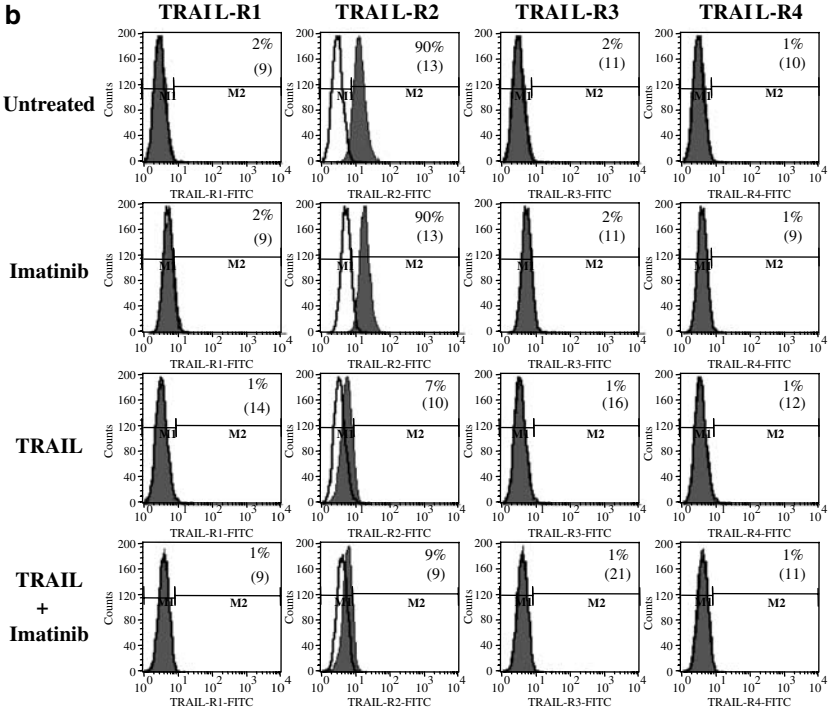

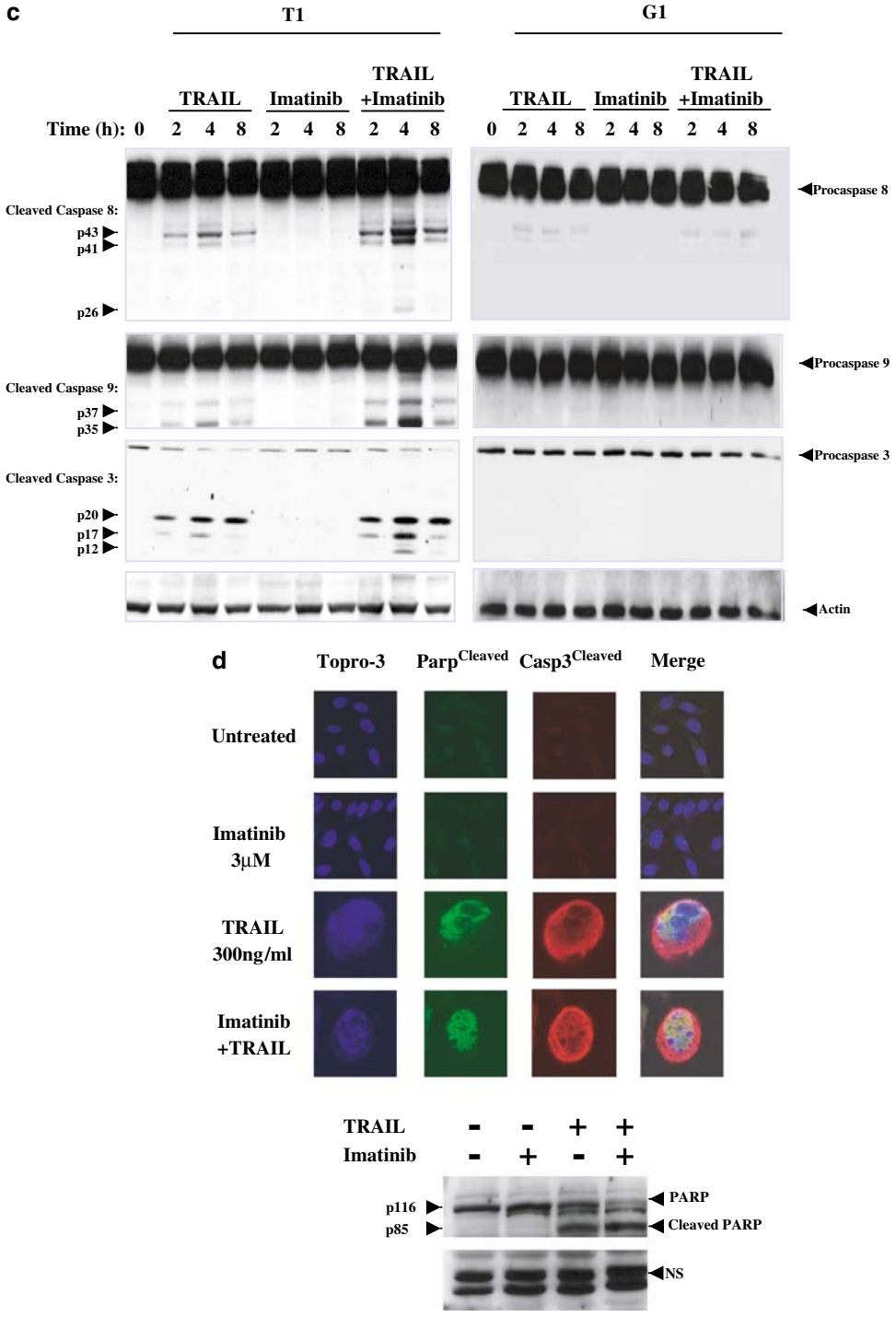

Figure 5 *Continued.*

not induce significant apoptosis in G1 and T1 cells (Figure 4e). Surprisingly, imatinib-TRAIL cotreatment did not induce apoptosis in G1 cells, but did induce TRAIL-induced apoptosis in T1 cells in a dose-dependent manner. This effect was maximal with 30 ng/ml of TRAIL and 10 μM of imatinib (P-value <0.02, 50% more apoptotic cells). More than 90% of cells were killed by treatment with a combination of 300 ng/ml TRAIL and 10 μM imatinib (33% more apoptotic cells). Thus, imatinib potentiates TRAIL-induced apoptosis in T1 cells by a mechanism involving the mitochondrial (or premitochondrial) pathway. Our results also suggest that the resistance of metastatic G1 cells to TRAIL-induced apoptosis is independent of c-kit activation.

In order to examine whether imatinib potentiates TRAIL-mediated apoptosis in other melanoma cells

lines, additional melanoma cell lines were used. Imatinib alone did not induce significant apoptosis in M10, MT10 and MG10 cells, at clinically relevant doses (Figure 4f). Treatment with TRAIL alone also failed to induce significant levels of apoptosis in M10 and MT10 cells, but it did markedly increase apoptosis levels in MG10 cells. Concomitant treatment with TRAIL and imatinib increased TRAIL-induced apoptosis in a dose-dependent manner in MG10 cells. Such potentiation of TRAIL-mediated apoptosis by imatinib was also observed in M10 and MT10 melanoma cells. Thus, imatinib sensitizes melanoma cells to TRAIL-mediated apoptosis.

Imatinib potentiates TRAIL-mediated apoptosis via an alternative pathway involving the enhancement of caspase activation

We investigated the mechanism by which imatinib increases the sensitivity of T1 cells to TRAIL, by evaluating the effect of this drug on the expression and activation of its own known targets, including c-ABL and PDGFRs. Neither of the cell lines tested expressed c-ABL or PDGFRβ. Treatment with imatinib or TRAIL, whether alone or in combination, did not modulate the expression or activation of these targets (Figure 5a). PDGFRα was expressed in T1 cells, but neither imatinib nor TRAIL, alone or in combination, modulated the activation of this protein. Thus, an alternative pathway must mediate the antitumor effects of imatinib. We then investigated whether imatinib potentiates the apoptotic effects of TRAIL, by modulating the levels of their receptors TRAIL-R1, TRAIL-R2, TRAIL-R3 and TRAIL-R4. Immunofluoresence analysis indicated that the treatment of either of the cells lines with TRAIL alone or with a combination of TRAIL and imatinib led to the complete abolition of TRAIL-R2 expression (Figure 5b). Imatinib alone did not increase TRAIL-R1 or TRAIL-R2 expression, demonstrating that TRAIL-mediated apoptosis in T1 cells was not enhanced by increases in the expression of these receptors.

We then investigated whether the effects of imatinib on TRAIL-mediated apoptosis in T1 cells involved the caspase cascade. Treatment with TRAIL alone or with a combination of TRAIL and imatinib-induced caspase 8, 9 and 3 processing in T1 cells at 2 h, with activity peaking 4 h after treatment (Figure 5c). TRAIL-induced caspase processing was more marked in the presence of imatinib. In contrast, imatinib alone did not affect caspase processing. No such processing was observed in G1 cells. As the additive effects of imatinib and TRAIL were correlated with caspase processing, we then investigated whether caspase processing was also correlated with caspase activation. Confocal microscopy and Western blotting showed that the cleaved forms of poly-ADP-ribose polymerase (PARP) and caspase 3 were observed following treatment with TRAIL alone or a combination of TRAIL and imatinib (Figure 5c).

Downregultion of c-FLIP$_L$ after imatinib treatment in T1 cells

c-FLIP proteins are critical regulators of death ligand-induced apoptosis, and the levels and activities of c-FLIP variants can modulate death ligand-induced caspase activation at the DISC (Barnhart *et al*., 2003; Ganten *et al*., 2004). To evaluate the correlation between c-FLIP expression, and TRAIL or imatinib sensitivity, we first checked the expression level of c-FLIP$_L$, c-FLIPs and Fas-associated DD kinase (FADD) in the T1 (Figure 6a) and G1 (Figure 6b) cell lines. Western blot analysis showed basal FADD protein levels were lower in G1 cells than in T1 cells. FADD production was not affected by either imatinib or TRAIL in either of the two cell lines, whereas combined treatment with both imatinib and TRAIL resulted in FADD downregulation in G1 cells only. Interestingly, c-FLIPs is not expressed in either T1 or G1 cells, whereas both cell lines constitutively express the similar levels of c-FLIP$_L$. Following imatinib treatment, c-FLIP$_L$ levels were downregulated more strongly in T1 cells than in G1 cells. Imatinib-TRAIL cotreatment increased c-FLIP$_L$ downregulation in T1 cells, at 8 h, whereas no such enhancement of downregulation was observed in G1 cells. These data show that c-FLIP$_L$ expression is affected by imatinib in T1 cell line.

We then investigated whether c-FLIP$_L$ interacted with the TRAIL-R2 receptor. An interaction between c-FLIP$_L$ and TRAIL-R2 was surprisingly observed in both T1 and G1 cells in the absence of TRAIL treatment (Figure 6c). This interaction between c-FLIP$_L$ and TRAIL-R2 was abolished by TRAIL stimulation in T1 cells and unaffected by such stimulation in G1 cells. These data suggest that the resistance of G1 cells to the apoptotic action of TRAIL may be at least partly due to defects in c-FLIP$_L$ release from TRAIL-R2, preventing procaspase 8 recruitment to the DISC and proteolytic cleavage.

c-FLIP$_L$ knockdown by siRNA is sufficient to sensitize melanoma cells to TRAIL-induced apoptosis

To show that c-FLIP$_L$ was indeed functionally involved in the sensitization of T1 cells to TRAIL by imatinib and the resistance of G1 cells to the apoptotic effects of TRAIL, we further performed siRNA experiment to knockdown c-FLIP$_L$ expression with two kinds of siRNA (S1 and S2). Western blot analysis indicated that c-FLIP$_L$ levels were significantly lower in cells transfected with these siRNA molecules than in cells transfected with the control siRNA (Figure 6d, upper panel). We then analysed the sensitivity of siRNA-transfected cells to TRAIL-mediated apoptosis. c-FLIP$_L$ downregulation sensitized T1 cells to TRAIL-mediated apoptosis, resulting in a sensitivity similar to that for cells subjected to imatinib pretreatment (P-value <0.00005; 33% more apoptotic cells) (Figure 6d, lower panel, left). In addition, c-FLIP$_L$ knockdown partly restored the sensitivity of G1 cells to the apoptotic action of TRAIL (P-value <0.005; $\sim$45% apoptotic cells) (Figure 6d, lower panel, right).

TRAIL-imatinib cotreatment alters the expression and translocation of Bcl-2 family members

Members of the Bcl-2 family are known to control the relative susceptibility of cells to apoptotic stimuli (Cory and Ridley, 2002). The p53/p21^{WAF1} pathway is also known to be a potent proapoptotic pathway (El-Deiry, 2001). We therefore investigated whether the enhancement of TRAIL-induced apoptosis by imatinib involved the modulation of p53/p21^{WAF1}, Bid, Bax, Bcl-2 and Bcl-X_L expression. Western blot analyses on whole-cell extract indicated that T1 cells had higher basal levels of Bcl-2, Bcl-X_L and Bid expression than of Bax expression (Figure 7a). Imatinib treatment led to the downregulation of Bcl-2 levels and the upregulation of Bax and p21^{WAF1} levels with respect to basal levels. We observed no change in p53, Bcl-X_L, Bid or cytochrome *c* levels (Figure 7a). The modulation of Bcl-2/Bcl-X_L, Bax, Bid and p21^{WAF1} expression after TRAIL treatment was not correlated with p53 levels. Interestingly, TRAIL-imatinib cotreatment downregulated the Bcl-2/Bcl-X_L proteins with respect to basal levels in untreated cells and upregulated Bax, increasing the Bax:Bcl-X_L ratio by a factor of 40, which was probably responsible for the observed activation of caspase 3 shown in the Figure 5c.

We then investigated whether the modulation of members of the Bcl-2 family was functionally relevant. For this purpose, we determined the subcellular distributions of Bcl-2, Bcl-X_L, Bax, Bid, and cytochrome *c* in treated T1 cells (Figure 7b). Imatinib alone slightly increased the amount of Bcl-2 and cytochrome *c* in the cytosolic fractions, but had no effect on the distribution of Bid or Bcl-X_L. TRAIL alone slightly increased the amount of Bcl-2 in the cytosolic fractions, but cotreatment with imatinib resulted in a more pronounced increase in the amount of this protein in the cytosol and a decrease in the amount of this protein in the mitochondrial fraction. Furthermore, the cotreatment of cells with imatinib and TRAIL resulted in a decrease in the amounts of Bcl-X_L and cytochrome *c* in the mitochondrial fraction, concomitant with cytochrome *c* release in the cytosolic fraction.

Cytochrome *c* release, and Bax and Bid translocation were further confirmed by immunostaining and confocal microscopy analysis (data not shown). Our results confirm that enhancement of the apoptotic effects of TRAIL by imatinib was independent of Bid translocation but correlated with cytochrome *c* release, and Bax translocation.

Imatinib alone downregulated Bcl-2 and induced its translocation into the cytosol. These data also indicate that the enhancement of TRAIL-mediated apoptosis by imatinib is independent of Bid translocation but correlated with cytochrome *c* release, Bax:Bcl-X_L ratio and Bax:Bcl-X_L/Bcl-2 translocation.

Discussion

In the present study, the comparison of T1 primary human melanoma cells and their metastatic counterpart, G1 cells, shows that T1 cells are more sensitive than G1 cells to TRAIL-mediated apoptosis. The resistance of G1 cells to TRAIL-mediated apoptosis was found to be independent of TRAIL receptor expression. Our experimental system may therefore be considered an appropriate *in vitro* model for investigating the molecular basis of the resistance of metastatic tumor cells to TRAIL-mediated apoptosis. We compared the gene expression profile of TRAIL-resistant metastatic and TRAIL-sensitive primary human cell lines, using the oligonucleotide microarray technique. Statistical analysis showed that resistance to TRAIL-mediated apoptosis was strongly correlated with expression signatures in this model. The genes identified as differentially expressed were associated with various biochemical and regulatory pathways, suggesting that a wide variety of intracellular signaling pathways are affected during the acquisition of resistance to TRAIL. Many of the differentially expressed genes identified in microarray analysis were found to be associated with ATP binding and some of these genes encoded protein tyrosine kinases. This group of kinases includes PDGFRs, colony-stimulating factor receptor, and Flt-3. The identified genes also included some encoding proteins involved in the MAPK and PI3K /AKT pathways. *KIT*, which codes for a type III receptor tyrosine kinase, was identified as a good candidate for connecting these pathways (Sattler and Salgia, 2004). *KIT* deregulation is thought to play a role in various tumors, including cutaneous melanomas (All-Ericsson *et al*., 2004). The ligand/c-kit axis may mediate solid tumor development

Figure 6 Imatinib decreased c-FLIP$_L$ expression when used alone and during TRAIL-induced cell death in T1 cells. T1 (**a**) and G1 (**b**) cells were incubated for 24 h with or without 3 μM imatinib and then with or without 300 ng/ml TRAIL for the indicated times. Cell lysates were subjected to SDS–PAGE, blotted and probed with the indicated antibodies. The corresponding nonspecific band (NS) levels are shown as loading controls. Densitometric analyses are represented in the graphs. (**c**) In the absence of TRAIL treatment, c-FLIP$_L$ is associated with the TRAIL-R2 receptor. T1 and G1 cells were treated with or without 300 ng/ml TRAIL for 1 h. The TRAIL-DISC was then immunoprecipitated with mAbs directed against TRAIL-R2. Possible nonspecific protein binding during immunoprecipitation was ruled out by incubating an equivalent amount of cell lysate with protein A-Sepharose beads after immunopreciptation with IgG1, the isotypic control of the TRAIL-R2 antibody. The immunoprecipitates were subjected to SDS–PAGE, blotted and probed with c-FLIP$_{L/S}$ antibody. Cell lysates were also analysed for c-FLIP$_{L/S}$, to show the specific band for c-FLIP$_{L/S}$. (**d**) Knockdown of endogenous c-FLIP$_L$ increased TRAIL-induced cell death in T1 cells and sensitized G1 cells to TRAIL-induced apoptosis. Cells were transfected with 28 nM of siRNA oligonucleotides designed to knockdown either a negative control (control), or two kinds of c-FLIP$_L$ (S1 or S2). After 72 h, the T1 cells and G1 cells were treated with TRAIL (300 ng/ml) for 5 h and 24 h, respectively. Upper panel: c-FLIP$_L$ expression was determined by Western blot analysis. The corresponding nonspecific band (NS) levels are shown as loading controls. The quantitative data indicated below each lane are densitometry values for c-FLIP$_L$ protein. Lower panel: Apoptosis was evaluated by $DiOC_6(3)$ and PI staining and FACS analysis. All data are expressed as means $\pm$ s.d. from two individual experiments (****$P<0.00005$; **$P<0.005$).

by autocrine or paracrine stimulation of the receptor or specific *KIT* mutation leading to the ligand-independent activation of the receptor (Sattler and Salgia, 2004). Our results indicate that the inhibition of melanoma cell line proliferation by a c-kit inhibitor, imatinib, is independent of c-kit expression. Our data also indicate that the resistance to TRAIL is independent of c-kit expression. This finding is consistent with the results of previous studies on human small-cell lung cancer (Decaudin *et al*., 2005) and various malignant cell lines (Uziel *et al*., 2005), indicating that the antitumor response of imatinib may be independent of c-kit expression. Uziel *et al*. (2005) showed that imatinib downregulates telomerase activity and inhibits

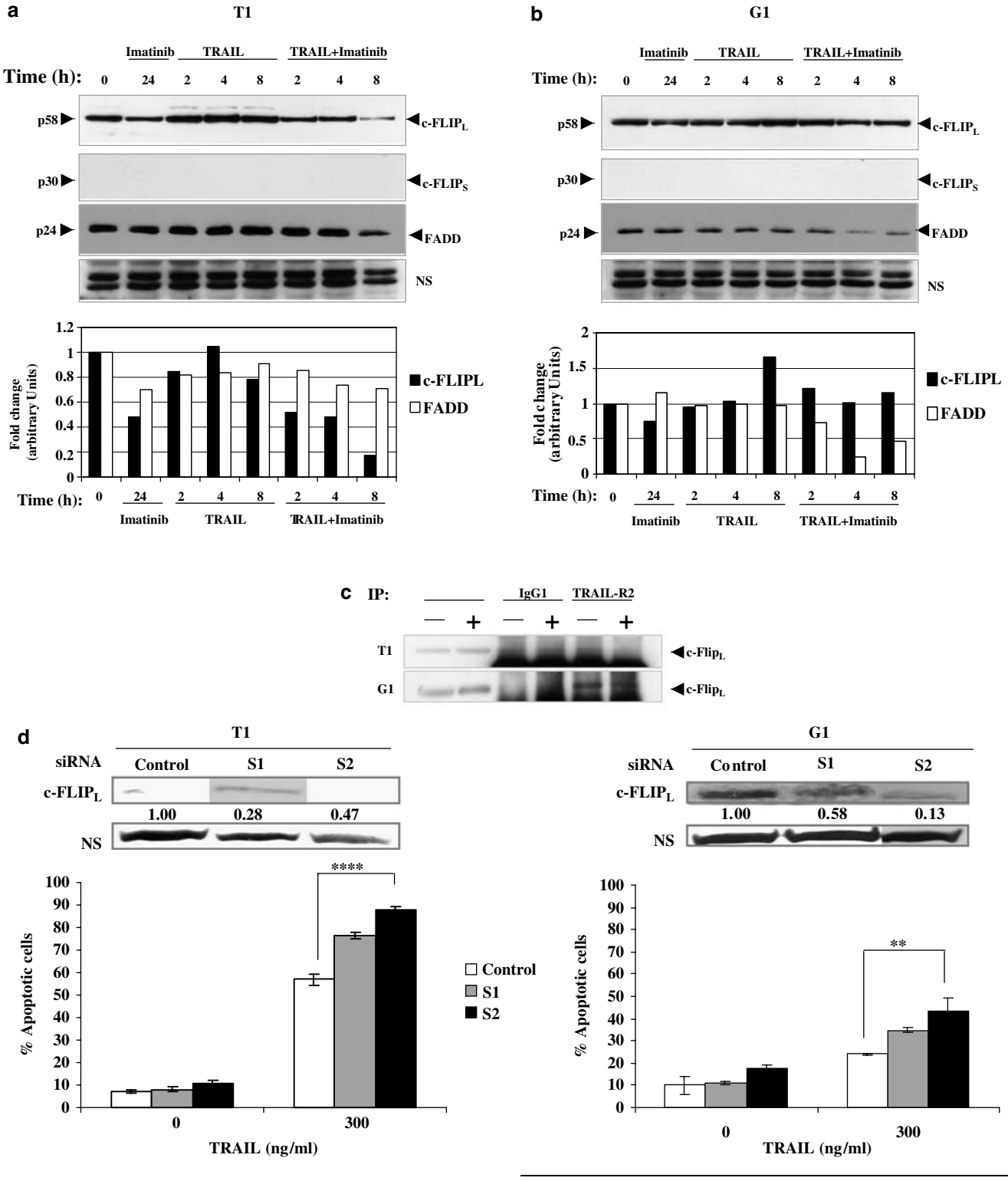

proliferation in telomerase-expressing cell lines. The inhibition of telomerase activity involves AKT dephosphorylation. The inhibition of Akt activity is known to enhance TRAIL-induced apoptosis (Nesterov *et al*., 2001; Kim and Lee, 2005). In our experimental model, Western blot analysis of Akt expression and phosphorylation showed that Akt was phosphorylated in both T1 and G1 cells and that treatment with TRAIL and/or imatinib treatment did not decrease Akt phosphorylation (data not shown). The inhibition of Akt activity could have accounted for the effect of imatinib on sensitivity to TRAIL, but our data rule out this mechanism in our experimental model. Imatinib treatment, alone or in combination with TRAIL, increased $p21^{WAF1}$ levels in T1 cells. This observation is consistent with the findings of previous studies on malignant cell lines (Pandiella *et al*., 2003), suggesting that imatinib may act via cell cycle arrest.

We also compared the effects of imatinib with those of a panel of tyrosine kinase inhibitors (AG490, PP2, type III tyrosine kinase inhibitors (TKI type III), and rapamycin) in T1 and G1 cells (data not shown). With the exception of rapamycin, most of the inhibitors tested efficiently enhanced TRAIL-induced apoptosis.

Treatment with imatinib at clinically relevant doses appears to be sufficient to inhibit cell proliferation, but insufficient to induce apoptosis, as shown by the absence of caspase activation, Bax or Bid translocation, mitochondrial damage and nuclear condensation. Our observations are not consistent with the data reported by Lefevre *et al*. (2004) showing the induction of cell apoptosis by imatinib in wild-type c-kit-positive cells only. This discrepancy could be due to the different *in vitro* models used in these studies. A combination of TRAIL and imatinib increased the inhibition of T1-cell growth, and increased the level of apoptosis. We initially thought that the inhibition of c-ABL and PDGFR might account for the effect of imatinib on TRAIL sensitivity, but the lack of expression or activation of these molecules after treatment in our experimental model rules out this mechanism. Our results are consistent with those of previous studies showing that the antitumor response of imatinib appears to be independent of PDGFR expression (Uziel *et al*., 2005). These findings demonstrate that imatinib has an additional cellular target, not necessarily corresponding to a known tyrosine kinase, inhibiting cell proliferation and potentiate TRAIL-induced apoptosis. The molecular mechanisms underlying the synergistic action of TRAIL and cytotoxic drugs are poorly understood, but it has been suggested that transcription of the genes encoding TRAIL-R1 and TRAIL-R2 is induced in certain tumor cell lines (Johnston *et al*., 2003). In our experimental model, imatinib did not appear to increase TRAIL receptor levels in melanoma cells, excluding the involvement of such a mechanism. In contrast, the observed decline in c-$FLIP_L$ levels following imatinib treatment indicates that c-$FLIP_L$ is a potential target of imatinib. Although the role of c-$FLIP_S$ as an inhibitor of DR-mediated apoptosis is well understood and resembles the activity of v-FLIP proteins (Thome *et al*., 1997; Krueger *et al*., 2001), the specific role of c-$FLIP_L$ in

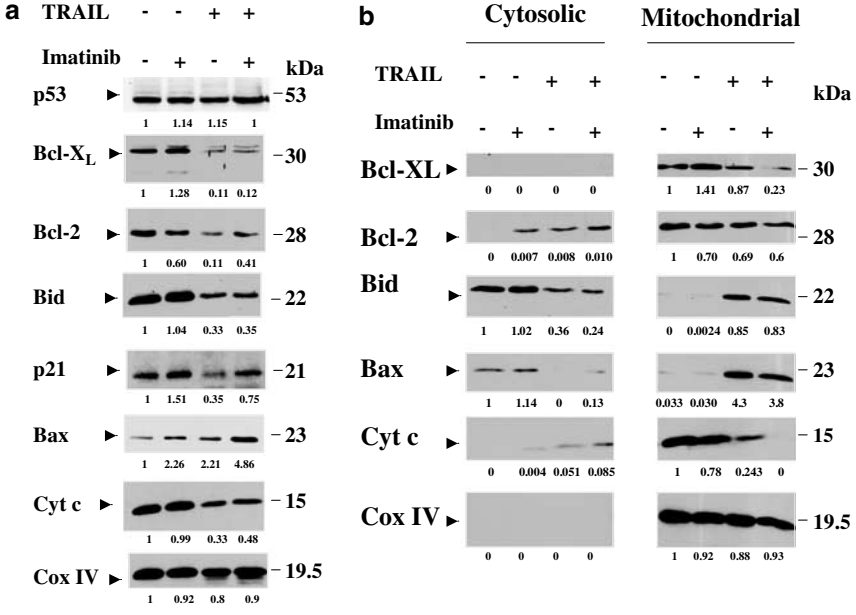

Figure 7 Combining TRAIL and imatinib increases Bax expression and translocation. (**a**) T1 cells were cultured in the presence or absence of imatinib (3 μM) overnight, and were then treated with TRAIL (300 ng/ml) or with a combination of imatinib and TRAIL for 4 h. Whole-cell lysates (30 μg) were subjected to SDS–PAGE, blotted and probed with antibodies, as indicated. Cox IV was used as the loading control. The quantitative data indicated below each lane correspond to densitometry values from two or three similar independent experiments. Taking into account the original cellular location of each protein, the untreated cell values were set to 1. (**b**) T1 Cells were cultured in the presence or absence of imatinib (3 μM) overnight, and were then treated with TRAIL (300 ng/ml) alone or a combination of TRAIL and imatinib for 4 h. Mitochondrial and cytosolic fractions were separated and subjected to SDS–PAGE, blotted and probed with antibodies, as indicated. Cox IV was used as control of the purity of the cytosolic fraction.

DR-mediated apoptosis remains unclear. The overexpression of c-FLIP$_L$ may either induce or inhibit apoptosis, depending on protein levels and cell type. In our model, the downregulation of c-FLIP$_L$ was correlated with the inhibition of proliferation and sensitization to TRAIL by imatinib. Specific c-FLIP$_L$ knockdown by siRNA significantly increased TRAIL-induced cell death in T1 cells and sensitized G1 cells to TRAIL-induced apoptosis. Our results are consistent with recent reports showing that c-FLIP$_L$ downregulation sensitizes resistant melanoma cells to TRAIL (Chawla-Sarkar *et al*., 2004). Moreover, c-FLIP$_L$ interacts with TRAIL-R2 in the absence of treatment. We found that the interaction between c-FLIP$_L$ and TRAIL-R2 was abolished in response to TRAIL stimulation in T1 cells, whereas this interaction was not affected in G1 cells. These data are supported by recent observations that c-FLIP$_L$ interacts directly with TRAIL-R2 and regulates TRAIL-induced apoptosis before formation of the DISC in HEK 293 and Jurkat cells (Jin *et al*., 2004). This mechanism differs from the current view that c-FLIP$_L$ prevents the formation of a competent DISC in a ligand-dependent manner, by interacting with FADD and/or caspase 8.

Sensitization to TRAIL by imatinib was correlated with a dramatic increase in Bax:Bcl-X$_L$ ratio and Bax:Bcl-X$_L$/Bcl-2 translocation. The signals activating Bax and Bak are not well known, but it has been suggested that tBid activates both proteins (Letai *et al*., 2002). As Bid can be cleaved by caspase 8, it has been suggested that Bid plays a crucial role in DR-induced apoptosis. We demonstrate here that Bid cleavage and translocation are not involved in melanoma cell sensitization to TRAIL by imatinib. These results are consistent with previous results showing that lymphocytes from Bid$^{-/-}$ mice display normal sensitivity to CD95-induced apoptosis, and that the lymphoid tissues of Bid$^{-/-}$ mice display no abnormalities. However, Bid$^{-/-}$ hepatocytes and fibroblasts show some resistance to DR-mediated apoptosis, indicating that Bid functions in a cell type-specific manner (Strasser, 2005). Bax overexpression is correlated with the extent of apoptosis and appears to be regulated independently of p53 protein levels. Cotreatment with imatinib enhanced TRAIL-induced apoptosis and increased the Bax:Bcl-X$_L$ protein ratio, affecting the mitochondrial pathway by $\Delta\Psi$m dissipation and the processing of caspase 8, 3 and 9. As imatinib does not itself induce caspase activation, the increase in caspase activation may result from a succession of interconnected amplification loops, as already reported (Strasser, 2005). Caspase 3 may thus proteolytically activate initiator caspases (caspase 8 and 9). Our data suggest that mitochondria and caspase cascade activation are involved in the imatinib-mediated sensitization of melanoma cells to TRAIL.

In conclusion, we found that resistance to TRAIL in G1 cells was correlated with constitutive c-FLIP$_L$ recruitment to the DISC and the inhibition of caspase 8, 3 and 9 processing. Moreover, c-FLIP$_L$ knockdown partly restored TRAIL sensitivity in TRAIL-resistant metastatic G1 cells, indicating that c-FLIP$_L$ levels and the interaction of c-FLIP$_L$ with TRAIL-R2 play key roles in determining the resistance of metastatic melanoma cells to TRAIL. TRAIL-sensitive primary T1 cells, which do not express c-kit, c-ABL and PDGFR, can be further sensitized to TRAIL-induced apoptosis by cotreatment with subtoxic doses of imatinib. We suggest that the apoptosis enhancement effect of combined treatment accelerates crosstalk between the extrinsic and intrinsic pathways via an amplification loop. In this loop, the apoptotic signal leads to caspase 8 activation, leading to caspase 3 activation, resulting in the further activation of caspase 8. Caspase 8 cleavage is followed by increases in apoptosome formation and caspase 3 activity, leading to the further activation of caspase 8. The apoptotic signal is amplified by changes in the ratio of Bax to Bcl-X$_L$ and the Bax/Bcl-2 to Bcl-X$_L$ mitochondrial translocation, leading to cytochrome *c* release. Simultaneously c-FLIP$_L$ interacts with TRAIL R2 in the absence of treatment, but this interaction was abolished by TRAIL treatment. Imatinib alone downregulated c-FLIP$_L$ in T1 cells. It also induced Bcl-2 downregulation and an increase in Bcl-2 levels in the cytosol. Imatinib also inhibited cell proliferation, increasing p21^{WAF1} levels.

The data reported here demonstrate the involvement of an alternative pathway in the antitumor activity of imatinib. It is tempting to speculate that the imatinib could be used to treat melanoma, in combination with TRAIL, independent of known targets. This combination may constitute a new therapeutic approach and should be evaluated in patients with melanoma.

Materials and methods

Reagents and antibodies

Recombinant human soluble APO2L/TRAIL (sTRAIL) was purchased from PeproTech Inc. (USA). AG490 (Cat No. 658401), rapamycin (Cat No. 553210), PP2 (Cat No. 529573), and tyrosine kinase receptor type III inhibitor (Cat No. 521232) were purchased from Calbiochem (USA). Protease inhibitors were purchased from Roche Applied Science (Mannheim, Germany). Bicinchoninic acid (BCA) protein assay reagent was obtained from Pierce (Rockford, IL, USA). 3-[(3-cholamido propyl)-dimethylammonio]-2-hydroxy-1-propanesulfonic acid (CHAPS) was obtained from Sigma (St Louis, MO, USA). mAbs directed against caspase 8 (clone 5F7) and caspase 9 (clone 4B4) were purchased from Immunotech (Marseilles, France). Anti-TRAIL-R mAb (clones M271, M413, M430 and M445, directed against TRAIL-R1,-R2,-R3, and-R4, respectively) were obtained from Immunex (Seattle, WA, USA). Antibodies against cleaved caspase 3 (clone 9661), c-kit, phosphorylated c-kit, c-FLIP$_{L/S}$, and phosphorylated c-ABL were purchased from Cell Signaling (Beverly, MA, USA). mAbs directed against PDGFRβ, phosphorylated PDGFRα and β, Bcl-2 (clone 100), Bax (clone N-20), actin (clone c-11), Bid (FL-195), p53 (DO-1) and Bcl-X$_L$ (S-18) were purchased from Santa Cruz (CA, USA). mAbs directed against c-ABL, p21^{WAF1} were obtained from Oncogene Research. mAbs directed against FADD, LCK, and cytochrome *c* for immunofluorescence staining (6H2.B4) and Western blotting (7H8.2C12) were obtained from PharMingen (San Jose, CA, USA). Anti-Cox IV mAb was from obtained from Molecular Probes (Eugene, Oregon, USA).

Antibodies against PDGFRα were purchased from Upstake Biotechnology (Lake Placid, NY, USA). Antibodies against PARP were purchased from BIOMOL Research Laboratories (Plymouth, PA, USA).

Cell lines

T1 and G1 are the melanoma cell lines derived from the primary lesion (T1) and from the metastatic lymph node (G1) of a single patient (FON), as previously described (Dufour *et al*., 1997). The M10, MT10 and MG10 additional melanoma tumor cell lines were derived from the primary lesion (M10), and from the metastatic lymph node (MT10) or from gastric metastasis (MG10) from another patient, as previously described (Carcelain *et al*., 1997).

The melanoma cells were cultured in RPMI 1640 medium supplemented with 10% FCS, 2 mM L-glutamine and 1 mM sodium pyruvate at 37°C in a humidified atmosphere containing 5% (T1, G1, M10 and MT10) or 7% (MG10) CO_2.

Cell death analysis

Cells were plated in a six-well plate at a density of 5×10^4 cells/well and incubated overnight. The medium was then replaced by either fresh medium (control medium) or by medium supplemented with various concentrations of TRAIL or imatinib or with a combination of these two compounds. Early apoptotic events were evaluated by annexin V labeling, using the annexin V-FITC propidium iodide (PI) assay kit (BD Biosciences, San Jose, CA, USA) according to the standard protocol.

Flow cytometry analysis

Cells were plated on a six-well plate, at a density of 5×10^4 cells/well and cultured overnight. Immunofluoresence analysis was carried out as previously described (Diarra-Mehrpour *et al*., 2004).

Purification, labeling, and hybridization of RNA

Total RNA was extracted from tumor cell lines using the RNeasy Mini kit (Qiagen, SA, Courtaboeuf, France), according to the manufacturer's protocol. The reference RNA was a pool of all RNA samples. In each experiment, fluorescent cRNA probes were prepared from an experimental RNA sample (coupled to Cy5) and a reference RNA sample (coupled to Cy3). Total RNA (5 μg) with a 28S/18S ratio greater than 1.8 was used to synthesize total cRNA with a linear amplification kit (Agilent, USA).

Labeling and hybridization were carried out as described by Array Express. Concentration and cy5/cy3 incorporation were determined with an Ultrospec (Amersham, Aylesbury, UK). Concentrations were adjusted to 100 ng/μl and the incorporation rate was 10–15 pmol/μg of cRNA. Microarrays carrying 60-mers (22 K human 2A) were provided by Agilent. Slides were scanned with an Agilent scanner in autofocus mode (resolution 5 μm). The accession number is E-MEXP-247.

Statistical analysis

Images were analysed with Feature Extraction software version A 6.1.1 from Agilent Technologies, with linear and lowness normalization based on local background. For clustering analysis, we used the Cluster and Tree initialization of the Genesis software developed at Graz University of Technology.

Primary analysis was carried out with the Rosetta Resolver software package. Hybridization quality was checked based on homogeneity of the distribution of the downregulated gene on the slide. Before clustering, we carried out both unsupervised PCA (Eriksson *et al*., 2004) and ANOVA to assess differences in the correlations between the groups and to select the most discriminating genes. Error-weighted and two-way ANOVA was used, with *P*-value $\leqslant 10^{-15}$ considered significant. The two factors included were cell line and TRAIL treatment (six levels: T1 or G1 without TRAIL, T1 or G1 with 0.2 or 1 μg/ml of TRAIL). Average linkage hierarchical clustering of an uncentered Pearson correlation similarity matrix was applied, using the Rosetta program. The Fatigo software package was used to assign genes to subgroups based on their biological process and molecular function (Al-Shahrour *et al*., 2004). Primary data are available from Array Express (http://www.ebi.ac.uk/arrayexpress/). The accession number is E-MEXP-247. Additional information is provided in the Supplementary Data.

TaqMan (Perkin-Elmer/Applied Biosystems, Foster City, CA, USA) real-time quantitative RT–PCR analysis

This analysis was carried out as previously described (Diarra-Mehrpour *et al*., 2004).

Cell proliferation

Cells were plated in a 96-well plate at a density of 5×10^3 cells/well and incubated overnight. After incubation with TRAIL, imatinib or a combination of the two, melanoma cells were incubated for 12 h in medium supplemented with 1 μCi/ml thymidine. The cells were frozen overnight at −20°C and then thawed at room temperature. Radiolabeled DNA was recovered on Unifilter-96 GF/C plates, using a manual harvester (Perkin-Elmer). Unifilter-96 GF/C plates were dried at 45°C for 4 h and microScint cocktail was then added. Radiolabeled DNA was quantified in a Topcount stacker NXT β-counter. Results are expressed as percentage proliferation inhibition (%) = (c.p.m. (untreated) − c.p.m. (treated))/c.p.m. (untreated). Values are expressed in c.p.m. and represent the mean of three replicates; s.d. never exceeded 9% of the mean.

Immunoblotting analysis of protein levels

This was done as reported (Wittnebel *et al*., 2005). Briefly, cells were lysed in an appropriate buffer containing 20 mM Tris-HCl (pH 7.5), 1% CHAPS, 150 mM NaCl, 10% glycerol, 1 mM Na_3VO_4, and a commercial protease inhibitor mixture (Complete Protease Inhibitor Mixture; Roche Molecular Biochemicals). Samples were placed on ice for 30 min and then centrifuged at $10\,000 \times g$ for 30 min at 4°C. The supernatants were collected. Equivalent protein extracts (30 μg) were resolved by SDS–PAGE, transferred to nitrocellulose membrane, and blotted with appropriate primary antibodies at a dilution of 1:1000. Peroxide-conjugated secondary antibodies were incubated with the membrane at a dilution of 1:2000. The membrane was then washed and the signal visualized by enhanced chemiluminescence (ECL, Western blotting Kit, Pierce). Densitometric analysis, including correction for background, was performed with NIH Image software.

Isolation of mitochondria and preparation of mitochondrial extracts

Mitochondria were prepared as previously described (Mikhailov *et al*., 2003; Poncet *et al*., 2004). Briefly, cells resuspended in homogenization buffer (300 mM sucrose, 10 mM *N*-tris[Hydromethyl]methyl-2-aminoethanesulfonic acid (TES), 300 μM ethylene glycol-bis(β-aminoethyl ether) *N*,*N*,*N*′,*N*′-tetraacetic acid) supplemented with a mixture of protease inhibitors were permeabilized by incubation at 4°C with 0.015–0.02% digitonin for 1–2 min and centrifuged at $15\,000\,g$ for 10 min at 4°C. The supernatant ('the cytosolic cell fraction') was recovered. The pellet was resuspended in homogenization

buffer and centrifuged at 900 *g* for 10 min at 4°C to remove nuclei and unbroken cells. The supernatant was recovered and centrifuged at 10 000 *g* for 10 min at 4°C and the pellet was used as the 'mitochondrial fraction'. The mitochondrial fraction was resuspended in homogenization buffer supplemented with 2% CHAPS, incubated on ice for 30 min, and centrifuged at 10 000 *g* for 30 min. Protein concentrations were determined using the BCA protein assay reagent. The fractions were analysed by Western blotting, as described above.

c-FLIP$_{L/S}$ analysis in DISC

T1 and G1 cells were incubated with or without TRAIL (300 ng/ml) for 1 h. Cells were washed with cold PBS and lysed by incubation on ice for 30 min in the same lysis buffer as used for immunoblot analysis. Insoluble debris was removed by centrifugation at 10 000 *g* for 30 min at 4°C. Equivalent amounts of protein (500 μg) extracted in 200 μl of lysis buffer were incubated with 0.5 μg of anti-TRAIL-R2 antibody or 0.5 μg of isotypic control IgG1 antibody overnight at 4°C, and then with 30 μl of protein A-Sepharose for an additional 3 h at 4°C. Immune complexes were collected by centrifugation for 5 min at 10 000 g, washed five times with lysis buffer, and released from the beads by boiling for 5 min in SDS sample buffer. Samples were resolved by SDS–PAGE, blotted and probed with c-FLIP $_{L/S}$ antibody.

siRNA transfection

The siRNAs used were designed with the Eurogentec RNA interference designer tool, for specific downregulation of the long form. The two sequences used were: (S1) GCU UGG CGC UCA ACA AGA A dTdT and (S2) GCC UGA UAA UCG AUU GCA U dTdT, together with a negative control siRNA purchased from Eurogentec. Subconfluent cells were transfected with siRNA in Opti-MEM, using the jetSI-ENDO™ reagent (from Polyplus-transfection™ Technologies, ILLKIRCH, France) according to the manufacturer's instructions.

Confocal scanning immunofluorescence microscopy

Cells were plated in a six-well plate at a density of 5×10^4 cells/well and incubated overnight. The medium was then replaced by either fresh medium (control medium) or by medium supplemented with TRAIL or imatinib or with a combination of these two compounds. We then washed the cells once with PBS and fixed them by incubation with 4% paraformaldehyde in PBS for 60 min. Cells were then rinsed three times with PBS. Sodium dodecylsulfate (0.1% in PBS) was used to permeabilize the cells for 10 min. The cells were washed three times with PBS and nonspecific-binding sites were blocked by incubation with 10% FCS in PBS for 20 min. Cells were then incubated for 60 min with a monoclonal antibody against cleaved PARP and cleaved caspase 3. Cells were washed three times with PBS and incubated with Alexa 488-conjugated goat anti-mouse IgG (Molecular Probes) secondary antibody. Cells were washed three times with PBS, and their nuclei were stained by incubation with Topro-3 (1/500 in PBS) for 5 min. Cells were washed three times and examined under an LSM 510 confocal microscope (Zeiss, Carl Zeiss LSM-510, Jena, Germany), as previously described (Diarra-Mehrpour *et al*., 2004; Wittnebel *et al*., 2005).

Abbreviations

Bax, BCL2-associated X protein; Bcl-2, B-cell leukemia/lymphoma 2; Bcl-X_L/BCL2L1, BCL2-like 1; Bid, BH3-interacting domain death agonist; DcR, decoy receptor; DISC, death-inducing signaling complex; DR, death receptor; FADD, Fas-associated DD kinase; FLICE, FADD-like interleukin-1 α-converting enzyme; c-FLIP, cellular FLICE-like inhibitory protein; IC50, concentration giving 50% growth inhibition; $\Delta\psi_m$, mitochondrial transmembrane potential; PARP, poly-ADP-ribose polymerase; PCA, principal component analysis; PDGFRs, platelet-derived growth factor receptors; PI, propidium iodide; TRAIL, tumor necrosis factor-related apoptosis-inducing ligand; TRAIL-R, TRAIL receptor.

Acknowledgements

We thank Philippe Dessen for his continuous help with microarray data analysis, Nazanine Modjtahedi for helpful discussions, Marie-Dominique Galibert for reading the manuscript and Catherine Gaudin and Thomas Robert for technical assistance. This work was supported by grants from INSERM, Association pour la Recherche sur le Cancer (grant 3520 to MD), and Ligue Nationale Contre le Cancer (Val de Marne 2002). Ahmed Hamaï is a recipient of a fellowship from cancéropole Ile de France and Fondation de France.

References

Al-Shahrour F, Diaz-Uriarte R, Dopazo J. (2004). *Bioinformatics* **20**: 578–580.
All-Ericsson C, Girnita L, Muller-Brunotte A, Brodin B, Seregard S, Ostman A *et al*. (2004). *Invest Ophthalmol Vis Sci* **45**: 2075–2082.
Ashkenazi A, Pai RC, Fong S, Leung S, Lawrence DA, Marsters SA *et al*. (1999). *J Clin Invest* **104**: 155–162.
Barnhart BC, Lee JC, Alappat EC, Peter ME. (2003). *Oncogene* **22**: 8634–8644.
Bittner M, Meltzer P, Chen Y, Jiang Y, Seftor E, Hendrix M *et al*. (2000). *Nature* **406**: 536–540.
Carcelain G, Rouas-Freiss N, Zorn E, Chung-Scott V, Viel S, Faure F *et al*. (1997). *Int J Cancer* **72**: 241–247.
Carr KM, Bittner M, Trent JM. (2003). *Oncogene* **205722**: 3076–3080.
Carroll M, Ohno-Jones S, Tamura S, Buchdunger E, Zimmermann J, Lydon NB *et al*. (1997). *Blood* **90**: 4947–4952.
Chawla-Sarkar M, Bae SI, Reu FJ, Jacobs BS, Lindner DJ, Borden EC. (2004). *Cell Death Differ* **11**: 915–923.
Clark EA, Golub TR, Lander ES, Hynes RO. (2000). *Nature* **406**: 532–535.
Cory GO, Ridley AJ. (2002). *Nature* **418**: 732–733.
Debatin KM, Krammer PH. (2004). *Oncogene* **23**: 2950–2966.
Decaudin D, de Cremoux P, Sastre X, Judde JG, Nemati F, Tran-Perennou C *et al*. (2005). *Int J Cancer* **113**: 849–856.
Desagher S, Osen-Sand A, Nichols A, Eskes R, Montessuit S, Lauper S *et al*. (1999). *J Cell Biol* **144**: 891–901.
Diarra-Mehrpour M, Arrabal S, Jalil A, Pinson X, Gaudin C, Pietu G *et al*. (2004). *Cancer Res* **64**: 719–727.
Druker BJ. (2002). *Oncogene* **21**: 8541–8546.
Dufour E, Carcelain G, Gaudin C, Flament C, Avril MF, Faure F. (1997). *J Immunol* **158**: 3787–3795.
El-Deiry WS. (2001). *Cell Death Differ* **8**: 1066–1075.
Eriksson L, Antti H, Gottfries J, Holmes E, Johansson E, Lindgren F *et al*. (2004). *Anal Bioanal Chem* **380**: 419–429.

Ganten TM, Haas TL, Sykora J, Stahl H, Sprick MR, Fas SC *et al*. (2004). *Cell Death Differ* **11**(Suppl 1): S86–S96.
Gross A, McDonnell JM, Korsmeyer SJ. (1999). *Genes Dev* **13**: 1899–1911.
Hasegawa J, Kamada S, Kamiike W, Shimizu S, Imazu T, Matsuda H *et al*. (1996). *Cancer Res* **56**: 1713–1718.
Heinrich MC, Griffith DJ, Druker BJ, Wait CL, Ott KA, Zigler AJ. (2000). *Blood* **96**: 925–932.
Hersey P, Zhang XD. (2001). *Nat Rev Cancer* **1**: 142–150.
Hodgkinson CA, Nakayama A, Li H, Swenson LB, Opdecamp K, Asher Jr JH *et al*. (1993). *Cell Death Differ* **74**: 395–404.
Ivanov VN, Bhoumik A, Ronai Z. (2003). *Oncogene* **p205722**: 3152–3161.
Ivanov VN, Hei TK. (2005). *Oncogene* **24**: 616–626.
Jin TG, Kurakin A, Benhaga N, Abe K, Mohseni M, Sandra F *et al*. (2004). *J Biol Chem* **279**: 55594–55601.
Johnston JB, Kabore AF, Strutinsky J, Hu X, Paul JT, Kropp DM *et al*. (2003). *Oncogene* **22**: 8356–8369.
Kelley SK, Harris LA, Xie D, Deforge L, Totpal K, Bussiere J *et al*. (2001). *J Pharmacol Exp Ther* **299**: 31–38.
Kim KM, Lee YJ. (2005). *Oncogene* **24**: 355–366.
Kroemer G, Zamzami N, Susin SA. (1997). *Immunol Today* **18**: 44–51.
Krueger A, Schmitz I, Baumann S, Krammer PH, Kirchhoff S. (2001). *J Biol Chem* **276**: 20633–20640.
Krystal GW, Honsawek S, Litz J, Buchdunger E. (2000). *Clin Cancer Res* **6**: 3319–3326.
LeBlanc HN, Ashkenazi A. (2003). *Cell Death Differ* **10**: 66–75.
Lefevre G, Glotin AL, Calipel A, Mouriaux F, Tran T, Kherrouche Z *et al*. (2004). *J Biol Chem* **279**: 31769–31779.
Letai A, Bassik MC, Walensky LD, Sorcinelli MD, Weiler S, Korsmeyer SJ. (2002). *Cancer Cell* **2**: 183–192.
Leverkus M, Neumann M, Mengling T, Rauch CT, Brocker EB, Krammer PH *et al*. (2000). *Cancer Res* **60**: 553–559.
Mikhailov V, Mikhailova M, Degenhardt K, Venkatachalam MA, White E, Saikumar P. (2003). *J Biol Chem* **278**: 5367–5376.
Muhlethaler-Mottet A, Bourloud KB, Auderset K, Joseph JM, Gross N. (2004). *Oncogene* **23**: 5415–5425.
Nesterov A, Ivashchenko Y, Kraft AS. (2002). *Oncogene* **21**: 1135–1140.
Nesterov A, Lu X, Johnson M, Miller GJ, Ivashchenko Y, Kraft AS. (2001). *J Biol Chem* **276**: 10767–10774.
Nimmanapalli R, Bhalla K. (2002). *Oncogene* **21**: 8584–8590.
Pandiella A, Carvajal-Vergara X, Tabera S, Mateo G, Gutierrez N, San Miguel JF. (2003). *Br J Haematol* **123**: 858–868.
Poncet D, Larochette N, Pauleau AL, Boya P, Jalil AA, Cartron PF *et al*. (2004). *J Biol Chem* **279**(7): 22605–22614.
Sattler M, Salgia R. (2004). *Leuk Res* **28**(Suppl 1): S11–S20.
Soengas MS, Lowe SW. (2003). *Oncogene* **22**: 3138–3151.
Strasser A. (2005). *Nat Rev Immunol* **5**: 189–200.
Taylor JR, Brownlow N, Domin J, Dibb NJ. (2006). *Oncogene* **25**: 147–151.
Thomas WD, Zhang XD, Franco AV, Nguyen T, Hersey P. (1998). *J Immunol* **161**: 2195–2200.
Thome M, Schneider P, Hofmann K, Fickenscher H, Meinl E, Neipel F *et al*. (1997). *Nature* **386**: 517–521.
Uziel O, Fenig E, Nordenberg J, Beery E, Reshef H, Sandbank J *et al*. (2005). *Br J Cancer* **92**: 1881–1891.
Walczak H, Miller RE, Ariail K, Gliniak B, Griffith TS, Kubin M *et al*. (1999). *Nat Med* **5**: 157–163.
Wang S, El-Deiry WS. (2003). *Oncogene* **22**: 8628–8633.
Weeraratna AT, Becker D, Carr KM, Duray PH, Rosenblatt KP, Yang S *et al*. (2004). *Oncogene* **23**: 2264–2274.
Wei MC, Lindsten T, Mootha VK, Weiler S, Gross A, Ashiya M *et al*. (2000). *Genes Dev* **14**: 2060–2071.
Wendt J, von Haefen C, Hemmati P, Belka C, Dorken B, Daniel PT. (2005). *Oncogene* **24**: 4052–4064.
Wittnebel S, Jalil A, Thiery J, DaRocha S, Viey E, Escudier B *et al*. (2005). *Eur Cytokine Netw* **16**: 123–127.
Yagita H, Takeda K, Hayakawa Y, Smyth MJ, Okumura K. (2004). *Cancer Sci* **95**: 777–783.
Yamaguchi K, Uzzo RG, Pimkina J, Makhov P, Golovine K, Crispen P *et al*. (2005). *Oncogene* **24**: 5868–5877.

Supplementary Information accompanies the paper on Oncogene website (http://www.nature.com/onc).